ISSN: 2639-7455

Research Article

Earth & Environmental Science Research & Reviews

Synthesis of Graphene Oxide Based Sodium Alginate Nanocomposites and their Application in Removal of Cr (VI) Ions from Coal Effluents

Prabha Raj[1*] and Rohit Kumar Bargah[2]

[1]*Department of Chemistry, Govt, Lahiri P.G. College, Chirmiri, Distt.-M.C.B., (C.G.), India. (Affiliated to Sant Gahira Guru University, Ambikapur, Sarguja (C.G.).*

[2]*Department of Chemistry, Govt. S.P.M. College, Sitapur, Sarguja, (C.G.).*

[*]Corresponding Author

Prabha Raj, Department of Chemistry, Govt, Lahiri P.G. College, Chirmiri, Distt.-M.C.B., (C.G.), India. (Affiliated to Sant Gahira Guru University, Ambikapur, Sarguja (C.G.).

Submitted: 2024, Dec 20; **Accepted:** 2025, Jan 24; **Published:** 2025, Feb 03

Citation: Raj, P., Bargah, R. K. (2025). Synthesis of Graphene Oxide Based Sodium Alginate Nanocomposites and their Application in Removal of Cr (VI) Ions from Coal Effluents. *Earth Envi Scie Res & Rev, 8*(1), 01-12.

Abstract

In the present study, graphene oxide-based sodium alginate nanocomposites have been used as an efficient low cast adsorbent to remove the concentration of toxic Cr (VI) ions from coal effluent. graphene oxide is prepared from sugarcane -bagasse and reacted with sodium- alginate and calcium-chloride to form the Na-Alg-Go composite. The developed composite was characterized by FTIR, XRD, TEM, particle size and zeta potential measurements. The adsorption experiments were carried out by batch contact method and the effect of the significant process parameter such as initial pH of solution, adsorbent dose, contact time and the initial Cr (VI) concentration were investigated on the metal ion removal capacity. The optimum adsorption of Cr (VI) on the Na- Alg-Go nanoparticles was observed at an initial pH value of 2.4±0.4. The maximum sorption capacity of Cr (VI) in coal effluent was found to be in between 100- 110 mg/g in comparison with std initial chromium (VI) solution in the range of 40-200 ppm at room temperature. The equilibrium sorption data fit satisfactorily to the Langmuir adsorption and Freundlich adsorption isotherm. The results suggest that adsorption is due to electrostatic attraction between chromate ions (HCrO -) and protonated surface of Na-Alg-Go composite and these has been efficaciously ecofriendly and economically applied for the removal of metal ion Cr(VI) and pollution from coal field effluent(Figure.1)

Keywords: Adsorbent, Graphene-Oxide, Sodium-Alginate, Coal Effluent, Cr (Vi) Metal Ion

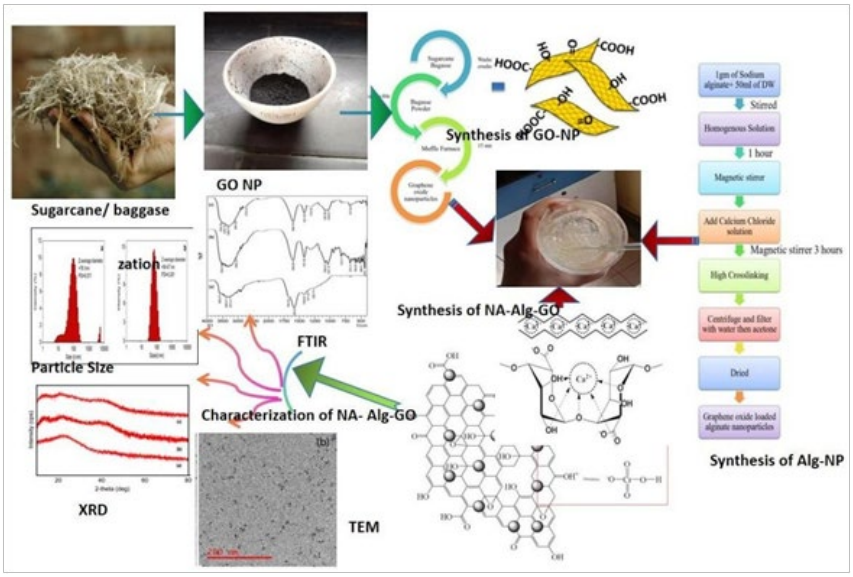

Figure 1: Graphical Abstract Synthesis and Characterization of Na-Alg-Go Nanocomposites

1. Introduction

Brutal human activities, such as mining and the discharge of industrialised waste materials into the environment, produce heavy metals, which are contaminants that do not biodegrade [1]. Over the course of the twentieth century, heavy metal contamination rose sharply [2,3]. Even at low concentrations and with just brief contact, heavy metal pollution has several detrimental physiological effects on ecosystems and organisms [4]. Heavy metal chromium is one of the most pervasive environmental contaminants and has very harmful effects on human health [5]. There is evidence that heavy metals and their compounds may cause cancer in humans and have negative impacts on metabolic systems [6]. Anaemia, elevated blood pressure, and interference with haemoglobin production are some of the most detrimental effects on human health [7]. The neurological system, liver, kidneys, and brain are particularly vulnerable. The careless release of industrial waste and mining are two examples of the many human activities that contribute to the pollution of our environment with heavy metals, which are not biodegradable [8,9]. Most of the chromite mines in the state of Orissa, India, discharge water containing between 2.0 and 5.0 mgL-1 chromium, and the effluents from the electroplating, ferrochrome, and leather tanning industries of Delhi and Aligarh (India) contain 50–100 mgL-1 of chromium (VI). So, chromium (VI) removal or reduction in mining and industrial effluents is important. In order to comply with these limits, it is necessary to propose appropriate treatment techniques that satisfy environmental as well as economic criteria [10, 11].

Any living thing has the potential to absorb chromium through their skin, lungs, or digestive tract. Conduct a comprehensive review of the literature on the topic of hexavalent chromium exposure in the environment, including both experimental and non-experimental research, to establish, evaluate, and prove the potential health risks to the exposed population [12]. Its toxicity is proportional to its potency and the way it is exposed. Trivalent chromium is present in many different forms in nature; it is an important trace element for human health, improves insulin action, and has a major role in the treatment of diabetes [13, 14]. On the other side, hexavalent chromium is harmful to human health when consumed in excess [15]. To synthesise nanoparticles, many methods have been documented, such as solvent deposition, controlled gellification, emulsification-diffusion, nanoprecipitation, solvent evaporation, and solvent polymerization [16]. One of these processes, controlled jellification, is highly sensitive to nanoparticle component concentrations; so, obtaining particles with nano-sized dimensions requires a high level of expertise.

The most common regeneration method for nanoparticle manufacturing is coprecipitation. Multiple compounds precipitating out of a solution at the same time is what this process is called. To prepare NPs, it is the most practical and cost-effective method. Two or more cations, which reside in a homogenous phase in the solution, are used in this approach. Uniform precipitation of different components can be achieved following the addition of the precipitant and the precipitation process.

Due of their long-term endurance and poor mechanical strength, sodium alginate sorbents are employed infrequently. There has been an improvement in mechanical characteristics when coupled with graphene oxide nanoparticles [17,18]. Hydrogen bonds can also develop between (Alg) and (GO) due to their structures. Alg-GO complexation should improve the mechanical and thermal properties of the composite material [19,20]. Composite porosity, electrostatic repulsion, and hydrogen bonding are all enhanced when combined with alginate and GO, which all dissolve readily in water and provide uniform solutions [21].

Thus the objective of this study was to synthesis and characterization of environment friendly graphene oxide based sodium alginate nanoparticles for the removal of Cr (VI) from coal effluent. for the purpose,the prepared graphene oxide impregnated sodium alginate nanoparticles were characterized by spectroscopic and microscopic characterization method like FTIR , SEM , TEM and XRD and used to investigate the removal of Cr(VI) metal ion from coal effluent.

2. Experimental

2.1. Study Area / Collection of Coalfield Effluents and Preparation of Synthetic Adsorbate Solution

The water sample collection process used to gather coal effluents from the Haldibadi underground mine in the Hasdevo field of Manendragarh, after treatment all of the effluent from coal mines is used for human consumption. In order to identity Cr(VI) metal ions sample of coal mines are Collected. Effluents were taken from the Haldibadi project in the Manendragarh distt M.C.B.(C.G.) India (Figure.2). The light black chilled effluent was collected in amber bottles with a temperature of around 20 degree Celsius. The American public health association APHA in the USA has established protocols for the proper storage of waste water samples and following the APHA guidelines the presence of toxic metals in the coal effluent were analysed and the observed results were compared with Std solution of hexavalent Cr (VI) in 100mL of double distilled water prepared by 0.2829g of potassium dichromate was dissolved to make a 1000 ppm chromium stock solution. This was diluted to meet experimental conditions [22].

Figure 2: Coal Effluents Sample Collection Picture and Map of Coal Filed Region

2.2. Materials

Merck, an Indian pharmaceutical company, supplied the sodium alginate and calcium chloride salts. Loba Chemie of Mumbai, India, supplied sulphuric acid (to activate the graphene oxide alginate nanoparticles), potassium dichromate (as an adsorbate), and 1,5-diphenylcarbazide (an indicator). As a solvent, double-distilled water was utilized throughout all tests.

2.3. Methods

2.3.1. Synthesis of Adsorbent Graphene Oxide Nanoparticles

Bagasse from sugarcane is one example of agricultural byproduct is used to prepare Graphene oxide nanoparticles. The residual fibre was removed after the juice was extracted. In order to make powder, the fibre was thoroughly ground and crushed. To get fine powder, this crushing and sorting operation was done several times. In a crucible, about half a gramme of sugarcane bagasse powder was heated to 500 degrees Celsius for 15 minutes before being transferred to muffle furnace warmed the sample further 15-20minutes at room temperature (Figure.3).

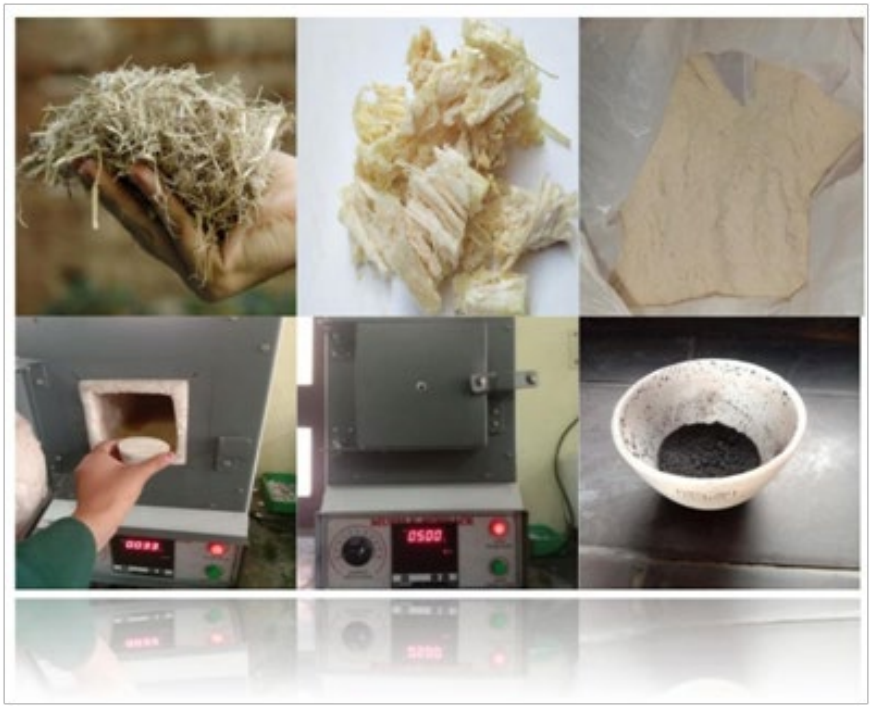

Figure 3: Various Working Images of Synthesis of Graphene Nanoparticles

2.3.2. Synthesis of Graphene Oxides Loaded Alginate Nano-composites

The nanoparticles of graphene oxide loaded alginate nanocomposites were prepared following an emulsion ionotropic gelation method by dissolving 1-gram sodium alginate in 50 ml deionized water in a 250 ml beaker. The solution was magnetically agitated for 1 hour since sodium alginate is water-soluble. After that, dissolve 0.5gm calcium chloride in 20 ml deionized water. After the sodium alginate solution was homogeneous, add the chloride solution to the system. In this case, the crosslinking is due to the presence of calcium chloride, which is utilized as a crosslinker and produces a polymer. To create a crosslinked polymer of sodium alginate, calcium chloride, and graphene oxide, the produced polymer was combined with 0.1 gm of graphene oxide and stirred with a magnetic stirrer for 1 hour. After centrifugation, the mixture was rinsed three times with ultrapure water and acetone. After filtering, the product was placed in a petri plate and baked overnight to make graphene oxide- loaded alginate nanoparticles (Figure 4).

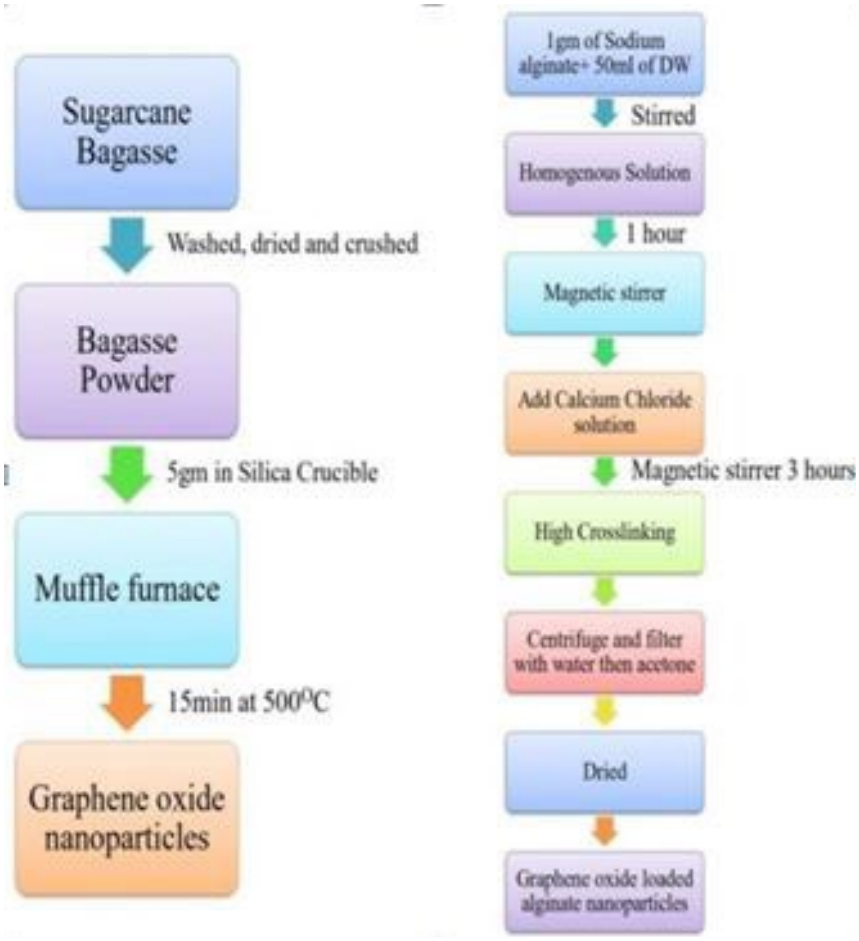

Figure 4: Schematic Diagram of Preparation of Graphene Loaded Alginate Nanoparticles

2.3.3. Adsorption Experiments

The studies were conducted using the batch contact method, which involves mixing specific volumes of adsorbate solution and adsorbent before conducting the tests. In a nutshell, a 20 mL effluents solution containing 0.01g of graphene alginate nanoparticles was maintained at a constant temperature and pH. A thermostat shaker (Rivotek, India) was used to shake the suspension for 15 minutes until it reached room temperature equilibrium. Spectrophotometric analysis of the concentration of Cr(VI) ions in the supernatant was performed after shaking stopped using a centrifuge from Remi, India, in accordance with the diphenyl carbazide technique. The complex formation may be shown by the following reaction (1),

$$2\,CrO_4^{2-} + 3H_4L + 8\,H^+ \rightarrow Cr(HL)_2^+ + Cr^{3+} + H_2L + 8\,H_2O \quad \text{.....1}$$

[H4L: 1, 5-Diphenylcarbazide] [H2L: Diphenylcarbazone]

The pH was modified by generating a medium acidic solution before adding the adsorbent, and the contact period, temperature, beginning Cr(VI) ion concentration, and content of Graphene Oxide loaded Alginate nanoparticles were varied. The adsorbent's removal efficiency was then examined at these levels. The amount of chromium(VI) adsorbed by the Na-Alg-GO nanoparticles and the percentage adsorption of chromium(VI) were calculated using Equations (2) and (3), respectively.

$$\% \text{ Removal} = C_i\text{-}C_e / C_i \times 100 \quad \text{.....2}$$

The amount of chromium adsorbed per unit mass of adsorbent qe (ppm/g) was obtained using the equation

$$q_e = (C_i - C_e) / m \times v \quad \text{.....3}$$

Where Ci and Ce denoted the initial and equilibrium Cr(VI) ion concentration (mg/L) respectively, m is mass of adsorbents and v volume of chromium solution.

3. Characterization of Prepared Adsorbent

The synthesized nanocomposites of Na-Alg-GO was characterized by different instrumental techniques. FTIR was used to identify the functional groups, while TEM, XRD, Zeta-potential and Size-distribution analysis were used to examine the morphology, surface structure, chemical characteristics, and crystalline features.

3.1. Interpretation by FTIR

Fourier transform infrared spectroscopy measurements were carried out with a Bruker Vertex70® spectrometer coupled to a Hyperion® microscope. The spectrum is ranging between 500 cm-1 to 4000 cm-1.

3.2. Interpretation by X-Ray Diffraction

X-ray diffraction studies of nanoparticles were carried out on the Rigaku MiniFlex X-Ray diffractometer. The diffraction data work collected from 10 to 80, 2θ with step size of 0.02 and counting time of 2s step-1. The average crystallite size of the nanoparticles estimated using scherrer's equation. The Scherrer equation is Dhkl = Kλ/(Bhklcosθ).

3.3. TEM Analysis

The particle size determination was carried out using the TEM images.Transmission electron microscopy(TEM) was performed by using a Morgagni-268-D transmission electron microscope with an acceleration voltage of 80.0 kv. The sample prepared for the TEM measurement were done by dispersing a drop of the sample solution on Formvar coated C grids. A TEM picture of the created graphene oxide, alginate, and graphene oxide loaded nanoparticles was taken to determine particle distribution and structural shape of the entrapped graphene nanoparticles.

3.4. Particle Size Distribution and Zeta Potential Measurements

The surface charge measurement is an important adsorption influencing parameter in toxic metal remediation. The size and surface charge properties of Na-Alg-Go nanoparticles determined in the zetasizer NanoZS 90 (Malvern instruments, UK). The zetasizer instrument works on the principle of dynamic light scattering (DLS) technique tom the size distribution curve of the particles. This DLS technique has also been used to determine the surface charges present on the synthesized nanomaterials.

4. Results and Discussion

4.1. FTIR Spectra Analysis of Graphene Oxide Nanoparticles

The FTIR spectra of Graphene oxide nanoparticles is shown in Figure.5(a). FTIR analysis was performed to examine the functional groups on the graphene oxide nanoparticles. The spectrum consists of vibrational groups of the Graphene that includes carbonyl (C = O), aromatic (C = C), carboxyl – (COOH), epoxy (C-O-C) and hydroxyl (O-H) groups. It is observed that a sharp peak at 3404 cm-1 corresponds to the carboxyl groups (O-H) due to the water molecules. The peak at 1691 cm-1 is due to ketone group (C=O) and the main graphitic domain of the peak at 1595 cm-1 is due to sp2 hybridization. The band at 1438 cm-1 reveals the C-O, 1282 cm-1 indicates the C O stretching of epoxy groups. The mode at 1020 cm-1 gives information about C-O stretching of alkoxy groups [23, 24].

4.2. FTIR Spectrum of Alginate Nanoparticles

The FTIR spectra of alginate nanoparticles crosslinked with calcium chloride is shown in Figure. 5(b). The FTIR spectrum of alginate nanoparticles display a number of absorption peaks. The broad peak around 3453 cm-1 is an indicative of existence of bonded hydroxyl group. The peak near 3543 cm_1 was caused by C—H stretching. The absorption peak at 2925 cm-1 represents the stretching band of the free carbonyl double bond from the carboxyl functional group[25]. The bands around 1046 cm-1 (C—O—C stretching) and 800 cm-1 (C—O stretching) present in the IR spectrum are attributed to its saccharide structure. In addition, the bands at 1594 and 1442 cm-1 are assigned to asymmetric and symmetric stretching peaks of carboxylate salt groups [26]. COO- stretching is split into asymmetric and symmetric C=O vibration. First peak observed at 1602 cm-1 (asymmetric stretching vibration of COO groups) and second peak at 1419 cm-1 (symmetric stretching vibration of COO groups). The bands at 1295 cm-1 were attributed to the C-O stretching vibration. The next peak, around 1084 cm-1, is related to C-O, C-C and to COC stretching vibrations. The strong and sharp peak at 1037 cm-1is also assigned to C-C and to COC vibrations these results indicate that the carboxylic groups of alginate are dissociated into – COO groups that can associate with trivalent cations through electrostatic interactions to form the egg box structure.

4.3. FTIR spectrum of Graphene Oxide Loaded Alginate Nanocomposites

The FTIR spectra of Graphene loaded alginate nanoparticles crosslinked with calcium chloride is shown in Figure. 5(c). In the spectrum a peak at 1606 cm-1 is observed due to the C=O stretching vibration of the carboxylic group of GO. Furthermore, the peak at 3369 cm-1 in Na-alg/GO attributed to OH stretching vibration broadened and shifted to smaller wavelengths. This phenomenon in the FTIR spectra adequately revealed that Na-alg and GO in the Na-alg/GO nanoparticles were tangled via strong hydrogen-bonding interactions between oxygen-containing group of GO nanoparticles and Na-alg chain.

For Na-alg/GO nanoparticle, the peak at 1606 cm-1weaker peak at 1421 cm-1 were attributed to the asymmetric and symmetric stretching vibration of the carboxylate group, respectively. These two peaks (1606 cm-1 and1421 cm-1) were the most useful characteristic peaks to investigate the ion crosslinking or exchange process. When the Na-alg and GO were crosslinked with Ca2+, the symmetric COO peak shifted to a higher wavenumber and the asymmetric COO peak shifted to a low wavenumber. The next peak, around 1087 cm-1, is related to C-O, C-C and to COC stretching vibrations. The strong and sharp peak at 1035 cm-1 is also assigned to C-C and to COC vibrations.

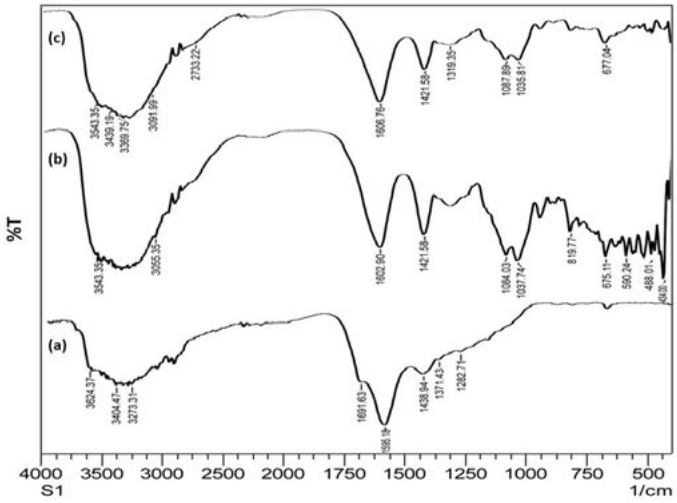

Figure 5: (a) FTIR spectra of Graphene oxide (b) FTIR spectra of Native Alginate Nanoparticles (c) FTIR Spectra of Graphene Oxide Loaded Alginate Nanoparticles

4.4. X-Ray Diffraction Analysis

The development of crystallinity in Graphene oxide is indicated by the well-defined X-ray diffraction patterns. Graphene oxide nanoparticles, native alginate nanoparticles, and alginate nanoparticles loaded with graphene oxide are all displayed in Figure. 6(a,b,c) together with their XRD spectra. Graphene oxide nanoparticles exhibit the distinctive peak at 23.2° in X-ray diffraction patterns (Figure.6(a)). The XRD patterns of the prepared alginate nanoparticles is shown in xray pattern in (Figure.6(b)). Alginate Biopolymer is an amorphous material however in the XRD spectra of alginate nanoparticles, the amorphous nature of alginate could not be observed as the particles were cross-linked with multivalent cations. Thus, the spectral pattern shown in Figure. 6(b) indicates low crystallinity whereas in Figure. 6(c) the appearance of two observable peaks on alginate surface at 21.4° and 37.1° suggests that graphene oxide has been loaded into the alginate nanoparticles. The obtained results agree with the reported standard data [27]. Equation (3) provides the Debye-Scherer formula, which was used to compute the mean grain size of the particles.

$$d = \frac{k\lambda}{\beta\cos\theta} \qquad \text{.....3}$$

The average grain size of graphene oxide impregnated Alginate nanoparticles is approximated at 6.8 nm, with d (mean grain size), k (form factor), β (diffraction angle broadening), and λ (1.54 Å) found.

The degree of crystallinity of graphene oxide alginate nanoparticles was calculated using Equation (4) to distinguish between amorphous and crystalline states.

$$Xc = \frac{Ac}{Aa + Ac} \times 100 \qquad \text{.....4}$$

The area of the crystalline phase is Ac, whereas that of the amorphous phase is Aa. Using the formula in equation (8), the nanoparticles' crystallinity has been determined. Native Alginate nanoparticles have a crystallinity of 43.8%,whereas Na-alg/GO nanocomposites have a crystallinity of around 67.5%.

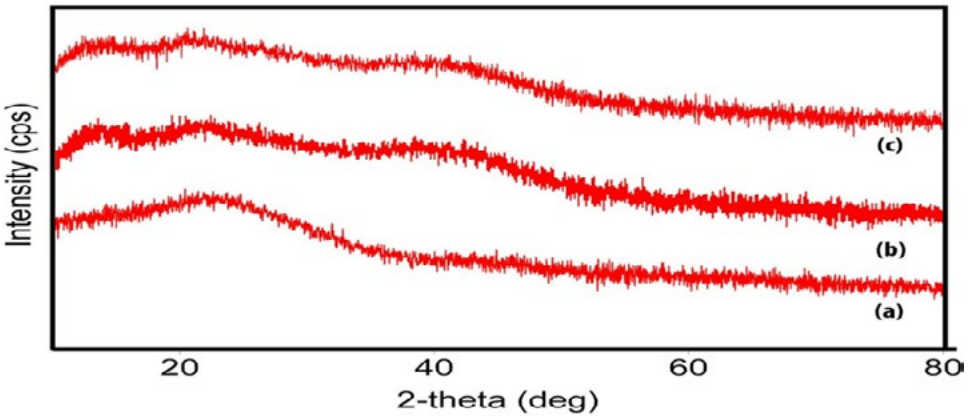

Figure 6: (a) XRD of Graphene Oxide (b) XRD of Native Alginate Nanoparticles (c) XRD of Graphene Oxide Loaded Alginate Nanoparticles

4.5. TEM (Transmission Electron Microscopy) Analysis

TEM offers a potent method for analyzing nanoparticle shape and size. When determining whether particles are suitable for use in metal adsorption applications, size—here meaning total diameter—is an important feature to consider. Due to colloidal methods to produce graphene sheets and device improvements in unsupported graphene, transmission electron microscopy (TEM) can now characterize suspended graphene at low magnification and atomic scale [28]. Most nanoparticles prefer to agglomerate, which lowers their surface charge, depending on their magnetic energy. Low metal adsorption with a high dosage of graphene-bound alginate nanoparticles may generate precipitation. Consequently, the size of the nanoparticles that are to be suggested for use in drinking water must be known.

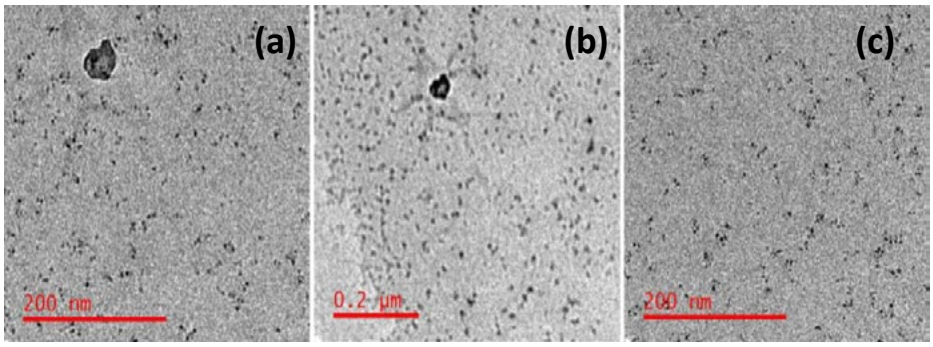

Figure 7: (a) TEM of Graphene Oxide (b) TEM of Native Alginate Nanoparticles (c) TEM of Graphene Oxide Loaded Alginate Nanoparticles

Images of nanoparticle clusters and individual particles were captured using transmission electron micrographs (TEMs), as shown in Figure.7 (a), (b), and (c), respectively, to study the size and shape of the prepared graphene oxide nanoparticles, alginate nanoparticles, and graphene loaded alginate nanoparticles. As shown in figure 7 (a, b), aggregated nanoparticles were 20–80 nm, while non-aggregated nanoparticles were 7–9 nm in Figure: 7 (c).

4.6. Particle Size Distribution and Zeta Potential Measurements

In order to find out the extent of agglomeration of graphene oxide alginate nanocomposites in the effluents solution, dynamic light scattering (DLS) measurements were carried out on synthesized nanocomposites at 25 °C and 80 °C as shown in Figure.8 (a, b). It may be observed that the particle size obtained from DLS measurements is 76.1 nm and 54.47 nm higher than the estimated from XRD broadening and TEM measurements. This may be due to the solvation effect of effluents the hydrodynamic diameter could be as higher the original diameter of the prepared nanoparticles or due to the presence of internal biomolecules in biomaterial alginate [29]. In order to have the testing samples ready, we followed this approach. The surface charge measurement is an important adsorption influencing parameter. As the Graphene–Alg nanoparticles were prepared by the physicochemical process, the electrostatic nature of these nanoparticles' changes with varying pH of the immersion medium. The surface charges were measured by suspending 0.1 g of the swollen Graphene–Alg nanoparticles. Produced nanoparticles of Cr (VI) adsorbed had Zeta potentials of -30 mV, -32 mV, and -48.2 mV, correspondingly. Graphene oxide derived from sugarcane bagasse has a negative surface charge because it contains ionized carboxyl, carbonyl, and hydroxyl groups from sucrose segments.

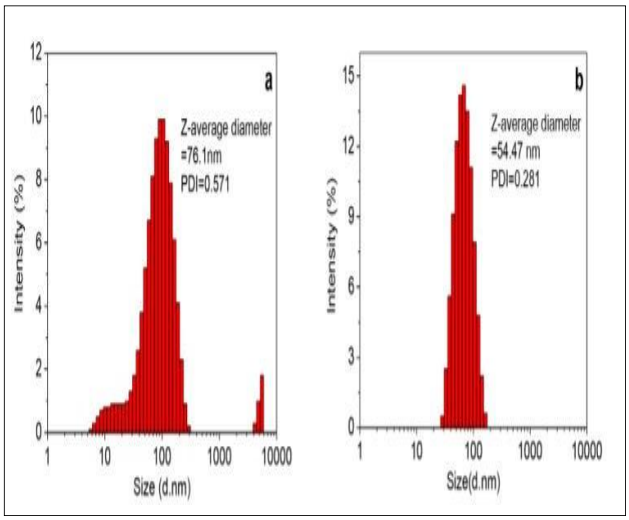

Figure: 8 (a,b): Particle Size Distribution of the Synthesized Graphene Oxide Loaded Alginate Nanoparticles at 25 °C (a) and 80 °C (b).

5. Results and Discussion

5.1. Batch Studies: (Effect of Agitation Time and Initial Metal Ion Concentration)

Equilibrium time is an important parameter for an industrial effluent treatment process. To test the concentration range of Cr(VI) metal in effluent sample initially batch studies performed on the std Cr(VI) solutions in different concentration range after that effluents were run under the selected range of metal concentration . The effect of agitation time on the removal efficiency of chromium(VI) at various initial std concentrations (40- 200ppm) by Graphene-Alg nanoparticles has been shown in Figure. 9 and Table 1. It was observed from the results that the adsorption of chromium(VI) ions is initially quite high, and with the lapse of time the adsorption lowers down very slowly leading finally to an equilibrium condition. The result indicates that a major fraction of chromium(VI) ions is adsorbed onto Graphene-Alg nanocomposites during the first 30-45 minutes while only a very small part of the additional adsorption occurs during the next one hour, reveals that during the initial time of the process there are plenty of readily accessible sites available for the increasing rate of adsorption.

As the time lapses the surface coverage increases, the rate of uptake becomes slower in latter stages, and ultimately an almost plateau region is attained when the surface become saturated. It may be noted from these

observations that the equilibrium is attained around 60 min. Effect of initial concentration on the percentage removal of Cr (VI) was studied at different initial concentrations by keeping other parameters constant. It was observed that with the increase in chromium initial concentration, the percentage removal of Cr(VI) decreases. This may be because at higher adsorbate concentration, the binding capacity of the adsorbent approaches saturation, resulting in decrease of overall percent removal.

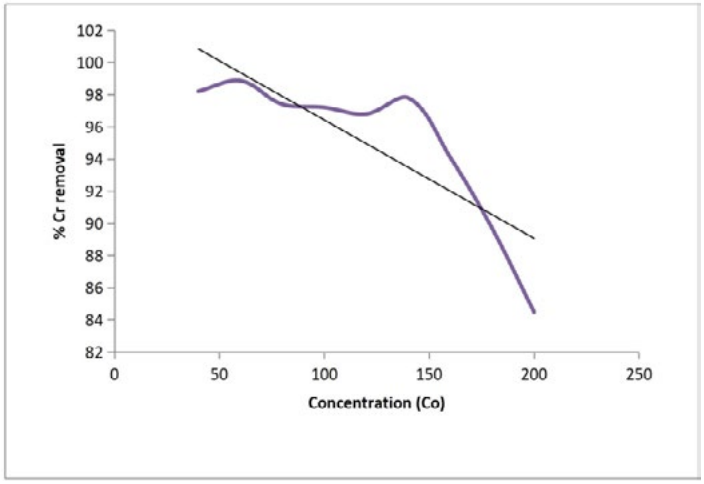

Figure 9: Effect of Concentration Ranging From 40-200 Ppm on the % Removal of Cr (VI)

S.No	Co	% Removal
1	40	98.2
2	60	98.86
3	80	97
4	100	97.2
5	120	96.8
6	140	97.2
7	160	95.12
8	180	89.7
9	200	84.5

Table 1: Data showing % removal values for concentrations ranging from 40-200 ppm, [m=0.1g], [v=10mL] [agitation time=90], [pH=2.4±0.4], temp=25°C±2]

5.2. Effect of Initial pH

The pH of the system controls the adsorption capacity of metal ions due to its influence on both the surface properties of the adsorbent, and the ionic forms of chromium present in the solution. Figure. 10 depicts effect of pH on the sorption of chromium ions onto the prepared graphene-Alg sorbent. The pH and concentration ranges used in this study indicate that HCrO4− in acidic medium and CrO42− in neutral and basic medium would be the predominant forms of chromium(VI). The studies were carried in the pH range of 2.4-9.5. Maximum chromium(VI) adsorption occurs when pH is 2.4 and chromium(VI) adsorption decreases as pH of the solution increases. Increasing the pH will shift the concentration of HCrO4− to its other forms. Thus, there are two possible reactions, as shown by Eqs. (5) and (6):

$$AOH_2^+ + HCrO_4^- \rightarrow AOH_2^+(HCrO_4^-), \text{ for pH} < \text{pH}_{ZPC} \quad \text{..... (5)}$$

or

$$AOH_2^+ + HCrO_4^- \rightarrow AHCrO_4 + H_2O, \text{ for pH} < \text{pH}_{ZPC} \quad \text{.....(6)}$$

where (AOH2+) symbolizes protonated adsorbent surface sites. These mechanisms are in agreement with the findings of previous studies on other adsorbents. The better adsorption at low pH by these graphene -Alg nanoparticles may be attributed to the large number of H+ ions present at low pH values which, in turn, neutralize the negatively charged adsorbents surfaces. This results in a strong electrostatic attraction between positively charged metal adsorbent surface (AOH2+) and HCrO4− leading to higher than initial adsorption. As the pH of the system increases, the number of negatively charged sites also increases while that of number positively charged sites decreases. Negatively charged surface sites on these graphene based adsorbents do not favor the adsorption of chromium(VI) ions due to the electrostatic repulsion. Furthermore, lower adsorption of toxic chromium(VI) ions in basic medium is also due the competition between excess OH− ions and the anions CrO_4− for the adsorption sites.

Thus, on the basis of different ionic species of chromium(VI) present in industrial effluents solutions, the maximum adsorption of chromium(VI) ions was observed at lower pH.

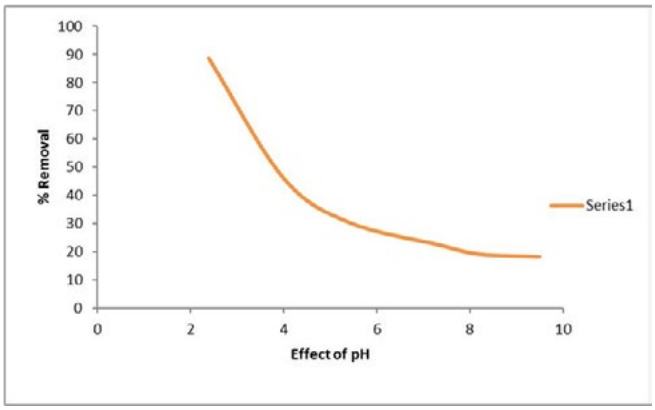

Figure 10: Effect of pH on Equilibrium Concentration Values of Cr (VI)

5.3. Effect of Adsorbent Dose

The effect of adsorbent dose on Cr (VI) removal at fixed initial Cr (VI) concentration is shown in Figure.11. It was observed that percentage removal of Cr (VI) increased with the increase in adsorbent dose. This can be explained by the fact that more mass available more the contact surface offered to the adsorption. % Removal and equilibrium concentration values for different adsorbent doses are summarized in Table 2 respectively.

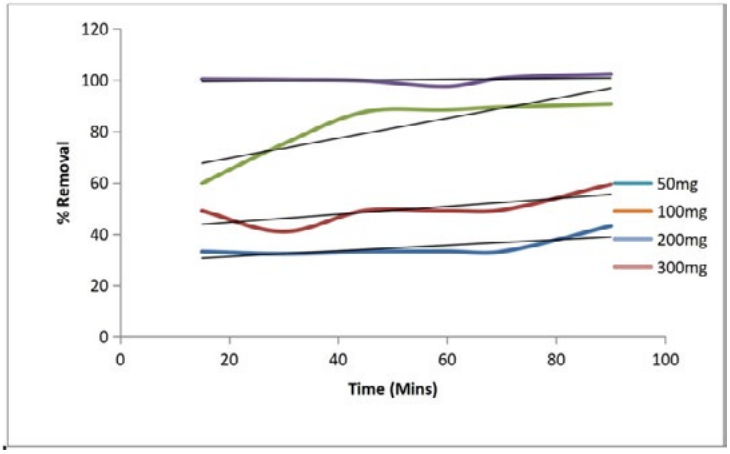

Figure 11: Effect of Adsorbent Doses 50-300mg on the % Removal of Cr(VI)

S.No	Time(mins)	50mg	100mg	200mg	300mg
1	15	33.13	49	59.8	100.4
2	30	32.33	41	75.2	100.2
3	45	33.2	49.1	87.7	99.8
4	60	33.21	49	88.5	97.6
5	70	33.16	49.35	89.5	100.8
6	90	43.15	59.4	90.8	102.4

Table 2: Data Showing % Removal Values for Adsorbent Doses 50-300mg At Different Time Intervals, [m=100mg], [v=10mL], [Ci=200ppm], [agitation time= 90 min], [pH=2.4±4], temp=25°C±2]

5.4. Effect of Temperature

The temperature effect was carried at 10oC, 25o C (Room Temp) and 50oC to study the influence of temperature on the Chromium ion capacity of graphene oxide-based alginate nanoparticles. Figure.12 and Table 3 Studies show that adsorption and removal increase at lower temperature. Increase in temperature lowers adsorption. This may be due weakening of adsorptive forces between alginate particles and Chromium ions. These results show that increase in temperature is unfavourable and decrease in temperature is a favourable factor for removal of Cr (VI) by alginate particles [30].

S.No	Time(mins)	10°C	25°C	50°C
1	15	8.97	4.9	8.74
2	30	9.43	4.1	8.74
3	45	9.81	4.91	9.07
4	60	10.01	4.9	9.69
5	70	10.18	4.935	9.78
6	90	10.23	4.94	10.78

Table 3: Data showing % Removal values for temperatures 10oC, 25oC and 50oC at different time intervals, [m=100mg], [v=10mL], [Ci=200ppm], [agitation time=90], [pH=2.4±4], temp=25°C±2]

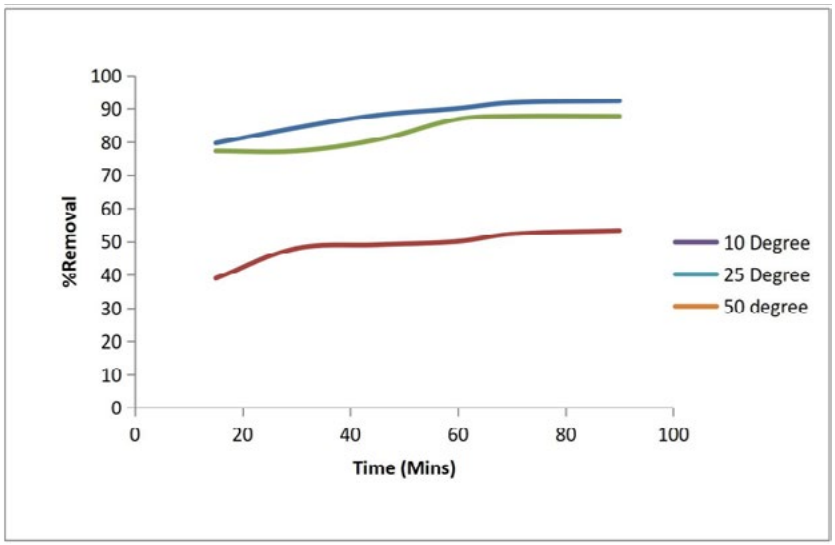

Figure 12: Effect of Temperature 10oC, 25oC and 50oC on the % removal of Cr (VI)

5. Conclusions

In this study a novel nanocomposite adsorbent comprising sodium-alginate nanoparticles impreagnated with graphene-oxide was successfully prepared for removing Cr (VI) from coal effluents. To prepare Graphene Oxide and alginate nanoparticles sugarcane bagasse and sodium alginate were used in the ratio of GO to sodium – alginate (10:1) with 6 % CaCl2 w/w solution to make the control set of Na-Alg-Go composite for efficient removal of Cr (VI) from coal effluents. The synthesized nanocomposites were characterized by FTIR, XRD, TEM and surface charge measurement techniques. It was observed that the sorption capacity increased with lowering pH, and the maximum sorption capacity of Cr (VI) in coal effluent was found to be in between 100-110 mg/g in comparision with std initial chromiunm(VI) solution in the range of 40-200 ppm at pH 2.4±0.4.

The sorption equilibrium and kinetics process fitted well to Langmuir, Freundlich and Lagergren models, respectively. The FTIR analysis show the impreagnation of graphene-oxide in to alginate nanoparticles. In the XRD studies native alginate nanoparticles have a % crystallinity of 43.8% whereas Na-alg/GO nanocomposites have a %crystallinity of around 67.5% indicate the development of moderate crytallinity on alginate nanoparticles and on graphene-oxide Na-Alg-Go nanoparticles. due to crosslinking with bivalent calcium ions and the mean grain size 20-80 nm or 7-9 nm of the Na-Alg-Go nanocomposite was in fair agreement with the TEM analysis results. The experimental results suggest that the Na-Alg-GO nanoparticles can be used as a potential adsorbent to remove heavy metals from aqueous solutions [31].

References

1. Fergusson, J. E. (1990). The heavy elements: chemistry. *Environmental Impact and Health Effects, 2*(1).
2. Duffus, J. H. (2001). "Heavy metals"–a meaningless term. *Chemistry International--Newsmagazine for IUPAC, 23*(6), 163-167.
3. H. Bradl, London: Academic Press; 200.
4. He, Z. L., Yang, X. E., & Stoffella, P. J. (2005). Trace elements in agroecosystems and impacts on the environment. *Journal of Trace elements in Medicine and Biology, 19*(2-3), 125-140.
5. Gallo, M. A., & Doull, J. (1996). History and scope of toxicology. Cassarett and Doull's Toxicology. The Basic Science of Poisons (Klassen CD, ed). 5th ed. New York: McGraw-Hill, 3-11.
6. Shallari, S., Schwartz, C., Hasko, A., & Morel, J. L. (1998). Heavy metals in soils and plants of serpentine and industrial sites of Albania. *Science of the total environment, 209*(2-3), 133-142.
7. J. O. Nriagu, Nature 1989 338:6210, 1989, 338, 47–49.
8. Arruti, A., Fernández-Olmo, I., & Irabien, Á. (2010). Evaluation of the contribution of local sources to trace metals levels in urban PM2. 5 and PM10 in the Cantabria region (Northern Spain). *Journal of environmental monitoring, 12*(7), 1451-1458.
9. Sträter, E., Westbeld, A., & Klemm, O. (2010). Pollution in coastal fog at Alto Patache, northern Chile. *Environmental Science and Pollution Research, 17*, 1563-1573.
10. Pacyna, J. M. (2023). Monitoring and assessment of metal contaminants in the air. In Toxicology of Metals, Volume I (pp. 9-28). CRC Press.
11. Bhattacharya, A. K., Naiya, T. K., Mandal, S. N., & Das, S. K. (2008). Adsorption, kinetics and equilibrium studies on removal of Cr (VI) from aqueous solutions using different low-cost adsorbents. *Chemical engineering journal, 137*(3), 529-541.
12. Thamilarasu, P., Sivakumar, P., & Karunakaran, K. (2011). Removal of Ni (II) from aqueous solutions by adsorption onto Cajanus cajan L Milsp seed shell activated carbons.
13. Sharma, D. C., & Forster, C. F. (1995). Column studies into the adsorption of chromium (VI) using sphagnum moss peat. *Bioresource Technology, 52*(3), 261-267.
14. Bansiwal, A., Pillewan, P., Biniwale, R. B., & Rayalu, S. S. (2010). Copper oxide incorporated mesoporous alumina for defluoridation of drinking water. *Microporous and Mesoporous Materials, 129*(1-2), 54-61.
15. Subbaiah, M. V., Vijaya, Y., Kumar, N. S., Reddy, A. S., & Krishnaiah, A. (2009). Biosorption of nickel from aqueous solutions by Acacia leucocephala bark: Kinetics and equilibrium studies. *Colloids and Surfaces B: Biointerfaces, 74*(1), 260-265.
16. Meenakshi, S. (1992). Studies on defluoridation of water with a few adsorbents and development of an indigenous defluoridation unit for domestic use.
17. Viswanathan, N., & Meenakshi, S. (2008). Enhanced fluoride sorption using La (III) incorporated carboxylated chitosan beads. *Journal of Colloid and Interface Science, 322*(2), 375-383.
18. Mohan, D., Singh, K. P., & Singh, V. K. (2008). Wastewater treatment using low cost activated carbons derived from agricultural byproducts—a case study. *Journal of Hazardous materials, 152*(3), 1045-1053.
19. Meenakshi, S., Sundaram, C. S., & Sukumar, R. (2008). Enhanced fluoride sorption by mechanochemically activated kaolinites. *Journal of hazardous materials, 153*(1-2), 164-172.
20. Kang, W. H., Kim, E. I., & Park, J. Y. (2007). Fluoride removal capacity of cement paste. *Desalination, 202*(1-3), 38-44.
21. Sundaram, C. S., Viswanathan, N., & Meenakshi, S. (2008). Uptake of fluoride by nano-hydroxyapatite/chitosan, a bioinorganic composite. *Bioresource technology, 99*(17), 8226-8230.
22. Wang, H., Chen, J., Cai, Y., Ji, J., Liu, L., & Teng, H. H. (2007). Defluoridation of drinking water by Mg/Al hydrotalcite-like compounds and their calcined products. *Applied clay science, 35*(1-2), 59-66.
23. Agarwal, M. Quest for black diamond: pollution from mines, power plants is choking chhattisgarh's coal hub.
24. S. Kumar, G. Bhanjana, A. Sharma, M. C. Sidhu and N. *Dilbaghi, CarbohydrPolym, 2014*, 101, 1061– 1067.
25. Namasivayam, C., & Yamuna, R. T. (1995). Adsorption of chromium (VI) by a low-cost adsorbent: biogas residual slurry. *Chemosphere, 30*(3), 561-578.

26. Kreuter, J. (1983). Evaluation of nanoparticles as drug-delivery systems. 1. Preparation methods. *Pharmaceutica Acta Helvetiae, 58*(7), 196-209.
27. Pandey, P. K., Sharma, S. K., & Sambi, S. S. (2010). Kinetics and equilibrium study of chromium adsorption on zeoliteNaX. *International Journal of Environmental Science & Technology, 7,* 395-404.
28. Hua, S., Ma, H., Li, X., Yang, H., & Wang, A. (2010). pH-sensitive sodium alginate/poly (vinyl alcohol) hydrogel beads prepared by combined Ca2+ crosslinking and freeze-thawing cycles for controlled release of diclofenac sodium. *International journal of biological macromolecules, 46*(5), 517-523.
29. Liu, Z., Suenaga, K., Harris, P. J., & Iijima, S. (2009). Open and closed edges of graphene layers. *Physical review letters, 102*(1), 015501.
30. Mukherjee, 4., Roy, M., Mandal, B. P., Dey, G. K., Mukherjee, P. K., Ghatak, J., ... & Kale, S. P. (2008). Green synthesis of highly stabilized nanocrystalline silver particles by a non-pathogenic and agriculturally important fungus T. asperellum. *Nanotechnology, 19*(7), 075103.
31. Kim, T. Y., Chung, J. H., Choi, S. Y., Cho, S. Y., & Kim, S. J. (2008, October). Adsorption characteristics of chromium ions onto composite alginate bead. I*n World Congress on Engineering and Computer Science, WCECS, San Francisco, USA.*